Received: 21 May 2021 | Revised: 4 December 2021 | Accepted: 9 February 2022

DOI: 10.1002/jbm.b.35042

RESEARCH ARTICLE

Society For Biomaterials | WILEY

Development of polycarbonate urethane-based materials with controlled diclofenac release for cartilage replacement

Andreia S. Oliveira[1,2,3] | Inês Ferreira[1,3] | Ana C. Branco[1,3,4] | João C. Silva[5] | Carolina Costa[1] | Pedro Nolasco[1] | Ana C. Marques[6] | Diana Silva[1,3] | Rogério Colaço[2] | Célio G. Figueiredo-Pina[3,4,7] | Ana P. Serro[1,3]

[1]CQE, Instituto Superior Técnico, Universidade de Lisboa, Lisbon, Portugal

[2]IDMEC e Departamento de Engenharia Mecânica, Instituto Superior Técnico, Universidade de Lisboa, Lisbon, Portugal

[3]CiiEM, Escola Superior de Saúde Egas Moniz, Monte de Caparica, Portugal

[4]CDP2T, Escola Superior de Tecnologia de Setúbal, Instituto Politécnico de Setúbal, Setúbal, Portugal

[5]IBB - Instituto de Bioengenharia e Biociências e Departamento de Bioengenharia, Instituto Superior Técnico, Universidade de Lisboa, Lisbon, Portugal

[6]CERENA, DEQ, Instituto Superior Técnico, Universidade de Lisboa, Lisbon, Portugal

[7]CeFEMA, Instituto Superior Técnico, Universidade de Lisboa, Lisbon, Portugal

Correspondence
A.P. Serro, CQE, Instituto Superior Técnico, Universidade de Lisboa, Lisboa, Portugal.
Email: anapaula.serro@tecnico.ulisboa.pt

Funding information
Fundação para a Ciência e a Tecnologia, Grant/Award Numbers: PD/BD/128140/2016, PTDC/CTM-CTM/29593/2017, SFRH/BD/145423/2019, UID/CTM/04540/2020, UIDB/00100/2020, UIDB/04585/2020, UIDB/50022/2020

Abstract

Hydrogels are very promising human cartilage replacement materials since they are able to mimic its structure and properties. Besides, they can be used as platforms for drug delivery to reduce inflammatory postsurgical reactions. Polycarbonate urethane (PCU) has been used in orthopedic applications due to its long-term biocompatibility and bio-durability. In this work, PCU-based hydrogels with the ability to release an anti-inflammatory (diclofenac) were developed, for the first time, for such purpose. The materials were reinforced with different amounts of cellulose acetate (CA, 10%, 15%, and 25% w/w) or carbon nanotubes (CNT, 1% and 2% w/w) in order to improve their mechanical properties. Samples were characterized in terms of compressive and tensile mechanical behavior. It was found that 15% CA and 2% CNT reinforcement led to the best mechanical properties. Thus, these materials were further characterized in terms of morphology, wettability, and friction coefficient (CoF). Contrarily to CNTs, the addition of CA significantly increased the material's porosity. Both materials became more hydrophilic, and the CoF slightly increased for PCU + 15%CA. The materials were loaded by soaking with diclofenac, and drug release experiments were conducted. PCU, PCU + 15%CA and PCU + 2%CNT presented similar release profiles, being able to ensure a controlled release of DFN for at least 4 days. Finally, in vitro cytotoxicity tests using human chondrocytes were also performed and confirmed a high biocompatibility for the three studied materials.

KEYWORDS
carbon nanotubes, cartilage replacement, cellulose acetate, drug delivery, hydrogel, polycarbonate urethane

1 | INTRODUCTION

Osteoarthritis (OA) is a chronic joint pathology characterized by the degradation of articular cartilage together with subchondral bone thickening, osteophyte formation, synovial inflammation, ligament degeneration, and capsule hypertrophy.[1,2] In the last years, its incidence has increased due to the population aging and the increasing prevalence of obesity.[3] Therefore, it is of utmost importance the study and development of new materials to replace damaged cartilage to maintain a longer active life. In order to solve this problem, surgical radical or conservative approaches can be considered, depending on the lesion stage of the patient.[4] Regarding invasive procedures, total joint arthroplasty is mostly recommended for patients suffering from end-stage lesions, where the cartilage tissue is entirely replaced by a simple mechanical device produced with materials such as titanium, cobalt-chromium alloys, alumina, and ultra-high molecular weight

polyethylene[5–8] The mechanical behavior of these materials is far from the human biological tissues, giving rise to several issues. For example, the differences in stiffness between the prosthetic material and the bone are responsible for stress shielding and consequent loss of bone tissue in the fixation areas.[9] Also, the polymeric material may suffer wear leading to the formation of debris that may accumulate in the bone-prosthesis interface resulting in osteolysis and consequently aseptic loosening of the implant,.[10,11] Hence, there is currently a tendency to perform the surgical procedures minimal invasive with the maximum preservation of the natural tissues, following a conservative approach. This can involve cartilage debridement aiming to remove damaged areas that are no longer functional, replacing them with healthy cartilage.[12] Another option is to use a synthetic biomaterial with structural and mechanical properties similar to natural cartilage that allows an efficient load transfer and cellular colonization. Hydrogels are attractive materials for this purpose due to their bi-phasic characteristics: they are composed of a polymeric network chain and water.[13] Their structure is quite similar to the cartilage, which is constituted by collagen fibers, proteoglycans, water, and chondrocytes.[14] Besides, the hydrogels' mechanical properties can match the ones present in cartilage. Finally, since hydrogels present high water absorption ability, they can be used for controlled hydrophilic drug administration at local level.[13–16] The rate of drug release from a hydrogel may depend on a variety of factors, such as the drug solubility, affinity to the polymeric chains, the water content of the hydrogel and its eventual erosion or degradation.[13] It shall be noted that the incorporation method of the drug into the hydrogel also affects the drug release profile.[17] In the postsurgical period, nonsteroidal anti-inflammatory drugs are usually prescribed to reduce pain. One of the most common is diclofenac (DFC), which decreases the formation of prostaglandin, blocks both cycloxygenase-1 (COX-1) and cycloxygenase-2 (COX-2).[18] It can be administrated orally or intravenously, being well absorbed, and has a rapid onset of action and a prolonged duration of analgesia.[19] The drug release at the local level constitutes an advantage since lower doses are needed, and the risk of secondary effects is reduced. It is especially useful in the first few days after surgery to favor recovery and a fast return to daily activities.

In the literature, some authors have studied the possibility of using hydrogels as potential materials for cartilage replacement with drug administration ability[20–22] Polycarbonate urethane (PCU, Figure 1) has attracted considerable attention in the orthopedic field, given its excellent mechanical properties (e.g., toughness, flexibility), long-term biocompatibility and bio-durability and resistance to hydrolytic and oxidative degradation.[23,24] PCU is more biocompatible and biostable than other kinds of polyurethanes (PUs), like poly(ether urethanes), due to the superior stability of the soft segments (polycarbonate) in the body.[25] It has been used for the production of meniscus implants,[26] cartilage substitutes,[27] the acetabular cup of hip replacement and spine stabilization, and cervical disc replacement devices.[24] For example, Elsner et al.[28] produced a fiber-reinforced, free-floating PCU meniscal implant and found that it could redistribute joint loads in a similar way to the natural meniscus, without compromising the integrity of the implant materials. Also, Linder-Ganz et al.[29] produced a PCU meniscal implant and evaluated the degenerative changes in the postsurgical period of a meniscectomy. They found that a PCU implant can offer chondroprotective capacity in the joint since it minimized the progression of degenerative cartilage changes over at least 6 months. In another work, Abar et al.[30] produced porous PCU structures by 3D-printing, to promote tissue integration of implants. They noticed that such structures could support NIH/3 T3 fibroblast cell line proliferation over 14 days. Kanca et al.[27] studied the in-vitro wear and friction behavior of PCU against articular cartilage. The observation of low friction coefficients (CoFs) and reduced cartilage counterface wear led them to conclude that PCU should be a promising candidate to be used in hemiarthroplasty, as long as the material was implanted in a region where migrating cartilage contact was achieved. However, as far as the authors know, it was never used in the form of hydrogels. The addition of reinforcement components to hydrogels is a strategy commonly used to improve their mechanical properties.[31,32] Cellulose acetate (CA) can be added to PCU for this purpose. It is a thermoplastic material produced by the esterification of cellulose and presents low toxicity, good thermal stability, good mechanical resistance, high flexibility and durability, chemical resistance, tailorable surface chemistry and great solubility in organic solvents[33–35] CA or other cellulose-based compounds may act as chain extenders or crosslinking agents when added to PU-based materials.[36,37] Their effect depends on factors such as the amount of CA added and the material's preparation stage when CA is added. Tang et al.[38] produced CA/PU composite nanofibers in a broad range of composition ratios by electrospinning and observed that the mechanical properties of the composite increased relatively to the initial mechanical properties of each component. No porosity was observed on the residual fiber surface, which indicates that the CA/PU nanofiber is a well-dispersed co-continuous nanocomposite material. Also, carbon nanotubes (CNT) have raised great interest as hydrogels reinforcement materials,[39,40] and for local drug delivery systems.[41] They present high chemical and thermal stability, ultra-light weight, and high-tensile strength.[42] Their use as a reinforcement agent has been demonstrated to improve not only the mechanical performance of the composites but also cell growth and proliferation without inducing inflammation or toxicity,.[41,43] CNTs' dispersion and their interfacial interaction with the polymer matrix determine the reinforced materials' performance. Their nanostructure and high interfacial area lead to the establishment of interactions that mainly result from van der Waals bonds.[44] Khang et al.[45] showed that CNT incorporation improves chondrocyte

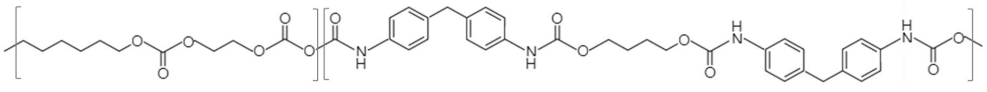

FIGURE 1 Typical chemical structure of polycarbonate urethane (PCU)

adhesion to the PCU, since the amounts of fibronectin (cell adhesion regulating protein) in PCU/CNT composite films increased due to the increase of hydrophilicity induced by the presence of CNT, which change the nanometric roughness. Bass[46] demonstrated that a mixture of ultra-soft PCU with CNT, resulted in polymers with better tensile mechanical properties. However, they also point out that several variables may influence the potential for CNT reinforcement in polymers, such as nanotube purity, functionalization, and nanotube-matrix interface, as well as the mixture process parameters.

This work aims to develop PCU hydrogels reinforced with CA or CNTs, with adequate properties for the replacement of damaged articular cartilage and ability to release in a controlled way an anti-inflammatory drug, that is, diclofenac. Different amounts of CA and CNT were added to PCU, and the equilibrium water content and compressive and tensile mechanical behavior of the obtained hydrogels were accessed. For the best performing materials, the morphology, hydrophilicity, and CoF against 316 L stainless steel were evaluated. These hydrogels were loaded with diclofenac, and the drug release profiles were obtained. Finally, cytotoxicity assays were performed for the most promising material.

2 | MATERIALS AND METHODS

2.1 | Materials

To produce PCU-based hydrogels, ChronoFlex® C™ 80A PCU (AdvanSource Biomaterials, molecular weight 1.1×10^5 Da), CA (Sigma-Aldrich, average molecular weight 3×10^3 Da), single-walled and double-walled carbon nanotubes (SW/DWNTs–purity>90 wt%, outer diameter 1–4 nm, length 5–30 μm) (Cheap Tubes Inc), N, N-dimethylformamide (DMF) (Chem-Lab) and pure acetone (José Manuel Gomes dos Santos [JMGS]) were used. For the preparation of the samples for scanning electron microscope (SEM) analysis, ethanol absolute anhydrous was obtained from Carlo ERBA and tert-butanol from PanReac. Hyaluronic acid (average molecular weight 1–2 million Da) to prepare the lubricant for the tribological tests was supplied by Carbosynth (Compton, Berkshire, UK), while phosphate buffered solution (PBS) was from Sigma-Aldrich. Diclofenac sodium (DFN, ≥98%, Sigma-Aldrich, Saint Louis, MO, USA) was used in the drug loading/release tests. Distilled and deionized water (DD water) ($\rho \geq 18\ M\Omega \cdot cm$) was obtained using a Milli-Q® water purification system (Integral 3 Millipore - Darmstadt, Germany). For the cytotoxicity tests, human chondrocytes were acquired from CELL Applications, Inc. (San Diego CA, USA), and the following reagents were used: high-glucose Dulbecco's Modified Eagle's Medium (DMEM: Gibco, Grand Island NY, USA) supplemented with 10% v/v fetal bovine serum (FBS, Gibco, USA), 1X MEM nonessential amino acids (Sigma, St. Louis MO, USA), 0.2 mM L-Ascorbic acid (Sigma), 0.4 mM L-Proline (Sigma) and 1% v/v penicillin–streptomycin (Pen-strep: Gibco). HCl (JMGS), (3-(4,5-dimethylthiazol-2-yl)-2–5 diphenyl tetrazolium bromide (MTT, Sigma), and isopropanol (Sigma) were also used in the in vitro cytotoxicity assay.

2.2 | Hydrogels preparation

PCU hydrogels were prepared by dissolving the PCU granules (15% w/w) in a mixture of acetone and DMF (50:50 v/v) at room temperature for 24 h and with magnetic stirring. The reinforcement with CA was carried out by mixing specific amounts of CA with PCU according to Table 1 (the total mass of solids was the same) and following the procedure mentioned above to ensure complete dissolution of the polymers. For CNT-reinforced hydrogels, CNTs were added to the prepared PCU solution and dispersed in an ultrasonic bath (VWR -USC300T, Leuven) for 4 h. The composition of the produced materials is shown in Table 1. The resulting polymeric solutions were poured immediately into borosilicate glass petri dishes and left in open air for 24 h. Thereafter, the plates were immersed in DD water to coagulate the solutions by exchanging the solvents. During this process, the DD water was exchanged twice a day for 3 days. The obtained hydrogels (thickness ≈ 2 mm, except otherwise stated) were cut with appropriate dimensions for the tests (discs of 6, 8, or 11 mm of diameter or test pieces with 4 mm of width and 20 mm of length) and kept in the hydrated state in sealed vials at room temperature till being used.

2.3 | Hydrogels characterization

2.3.1 | Equilibrium water content and swelling capacity

The hydrated hydrogels (discs with diameter 8 mm) were weighted in order to obtain the hydrated weight (w_{h1}). Then the samples were dried at 40°C for 24 h and thereafter submitted to vacuum for 48 h and weighed again to obtain the dry weight (w_d). The equilibrium water content (%EWC) was calculated through the following equation:

$$\%EWC = \frac{W_{h1} - W_d}{W_{h1}}, \quad (1)$$

In order to evaluate the reversibility of the swelling process after drying, the previous dried samples were rehydrated in water until they reached a constant weight. (w_{h2}). The swelling capacity (%SC) was determined using the expression:

$$\%SC = \frac{W_{h2} - W_d}{W_d}, \quad (2)$$

Materials were characterized in triplicate.

2.3.2 | Mechanical properties

To determine the tensile and compression properties, an Instron® 5566 Universal Testing machine (Instron Corporation), with a load cell

TABLE 1 PCU, PCU/CA and PCU/CNT samples composition

Samples	Acetone (ml)	DMF (ml)	PCU (mg)	CA (mg)	CNT (mg)
PCU	6.1	6.1	3750	–	–
PCU + 10%CA			3375	375	–
PCU + 15%CA			3188	563	–
PCU + 25%CA			2813	937	–
PCU + 1%CNT			3712	–	38
PCU + 2%CNT			3675	–	75

of 10 kN, controlled through the software Bluehill® 2, was used. Hydrated discs (diameter 11 mm) were compressed at 0.1 mm/s until reaching a maximum compressive stress of 8.42 MPa. Tensile tests were carried out at the same test speed until rupture. Experiments were performed at room temperature. A minimum of five repetitions was done in each case. Both the tangent compressive and tensile modulus were calculated from the slope of obtained stress–strain curves in each point. For compression tests, the absorbed energy was calculated by integrating the stress–strain curve until a deformation of 60%. For tensile tests, the elongation-to-break, toughness, and ultimate tensile strength (UTS) were determined.

2.3.3 | Morphology

PCU, PCU + 15%CA, and PCU + 2%CNT samples were analyzed in a Hitachi S-2400 SEM at 15 kV. Discs with 11 mm of diameter were previously dipped in liquid nitrogen, sectioned in half, and immersed in DD water at room temperature. Dehydration was done following a procedure described by Bodenberger et al.[47] for preparation of sensitive samples for SEM analysis, which involves the sequential immersion of the samples in ethanol 70% vol, ethanol 96% vol, and ethanol 100% vol, 3 × 15 min each step. Afterward, the samples were submerged in tert-butanol at 40°C for 3 × 15 min, cooled to 4°C, and then dried in a low-vacuum oven for 24 h.[48] Before SEM observations, the materials were coated with a metallic film of gold and palladium with 20 nm of thickness in a Quorum Technologies sputter coater and evaporator.

2.3.4 | Wettability

The hydrophilicity of PCU, PCU + 15%CA, and PCU + 2%CNT samples was accessed through the measurement of the water contact angle by using the captive bubble method. Hydrated discs with 11 mm of diameter were fixed to a platform and placed downwards inside a liquid cell with quartz windows filled with DD water. Air bubbles (3–6 μL) were generated with a micrometric syringe with an inverted needle under the material's surface. Images were acquired for 10 min at predefined time intervals using a video camera (JAI CV-A50, JAI A/S, Grosswallstadt, Germany) connected to a frame grabber (DT3155, Data Translation, Norton, MA, USA) and coupled to an optical microscope (M3Z, Wild, Heerbrugg, Switzerland). ADSA-P (Axisymmetric Drop Shape Analysis Profile) software was used to perform image analysis. For each material, at least eight bubbles were done.

2.3.5 | Friction coefficient

The CoF of the materials PCU, PCU + 15%CA and PCU + 2%CNT was evaluated using a tribometer (TRB^3, Anton Paar, M.T. Brandão, Porto, Portugal). The tests were carried out in a HA solution (3 mg/ml, prepared in PBS), at room temperature, in a ball-on-plate configuration, in linear reciprocating motion, using a 6 mm diameter 316 L stainless steel (SS) ball (Luis Aparicio SL, Barcelona, Spain) as counterbody. Two loads (5 and 10 N) were tested, and the following parameters were set: total distance of 10 m (cyclic path of 8 mm), maximum linear speed of 31.4 mm/s, and frequency of 1.25 Hz. The tests were done in triplicate for all materials.

2.3.6 | Drug loading and release

PCU, PCU + 15%CA, and PCU + 2%CNT hydrated discs with 6 mm diameter were individually immersed in 3 ml of DFN solution (2 mg/ml) and sterilized at 121°C for 30 min at 1 bar in an autoclave. Thereafter, they were left for 7 days at 37°C under shaking (VWR Mini Incubation Shaker) at 180 rpm. After this period, the loaded discs were removed from the drug solution and wiped with absorbent paper to remove the excess solution from the samples' surface. For the drug release experiments, they were immersed in 3 ml of PBS and placed at 37°C on an agitator at 180 rpm for the drug release experiments. Aliquots of 300 μL were collected at predefined intervals for 48 h, and the volume removed was replaced with fresh PBS. The concentration of DFN in the release solution was determined using a UV–Vis spectrophotometer (Multiskan™ GO Microplate Spectrophotometer, Thermo Fisher Scientific, Kandel, Germany) by measuring the absorbances at a wavelength of 276 nm. A calibration curve was previously obtained using solutions of known concentration. The total amount of drug loaded into the samples was determined by extraction with ethanol. Each sample was immersed in 3 ml of ethanol. At predetermined times, the supernatant solution was analyzed by UV–Vis spectroscopy, as referred above, and replaced with fresh ethanol. The procedure was performed until no more drug could be extracted. The cumulative amount was determined.

2.3.7 | Cytotoxicity evaluation

Disks with 10 mm diameter of PCU, PCU + 15%CA, and PCU + 2% CNT were submitted to biocompatibility tests with human chondrocytes, according to the ISO-10993-12 guidelines.[49] The samples were previously sterilized at 121°C for 30 min at 1 bar in an autoclave. Direct contact and indirect extract (lixiviates) tests were performed. For both assays, the cells were seeded on tissue culture polystyrene (TCPS) 24-well plates with a density of 1.2 x 105 cells per well and cultured for 24 h at 37°C and 5% CO_2 to achieve a confluent monolayer. Negative control corresponded to the cells cultured on TCPS in culture medium, while positive control was latex. For the direct contact test, the hydrogels (n = 3) were placed over the cells monolayer and incubated for 48 h at 37°C and 5% CO_2. An inverted optical microscope (LEICA DMI3000B, Leica Microsystems, Germany) equipped with a digital camera (Nikon DXM1200F, Nikon Instruments Inc., Japan) was used to qualitatively assess the cells' viability and their morphology. For the indirect test, material extracts were obtained by incubating the hydrogels (n = 5) in culture medium (3 cm^2 of samples' surface area/ml) for 24 h, at 37°C and 5% CO_2. Then, the medium was collected and was poured onto the cells' culture plates which were kept for 48 h at 37°C and 5% CO_2. Afterward, the medium was removed, and the MTT assay (In Vitro Toxicology Assay Kit, MTT based, Sigma, MO, USA) was performed according to the manufacturer's guidelines. For that, the cells were incubated in the MTT solution (yellow, 1 mg/ml) for 4 h at 37°C. The violet formazan product produced in the MTT metabolic reduction by the viable cells was dissolved in 0.1 M HCl solution previously prepared in isopropanol. The percentage of viable cells for the different samples was calculated from absorbance measurements (done in triplicate) of the resultant solution performed in a microplate reader (Infinite M200 PRO, TECAN, Switzerland) at 570 nm, using as reference the values obtained for the negative control.

2.4 | Statistical analysis

Statistical analysis was carried out using Excel Statistical Tools. Shapiro–Wilk test was performed to verify the normality of the results. One-way analysis of variance (ANOVA) and student *t*-test

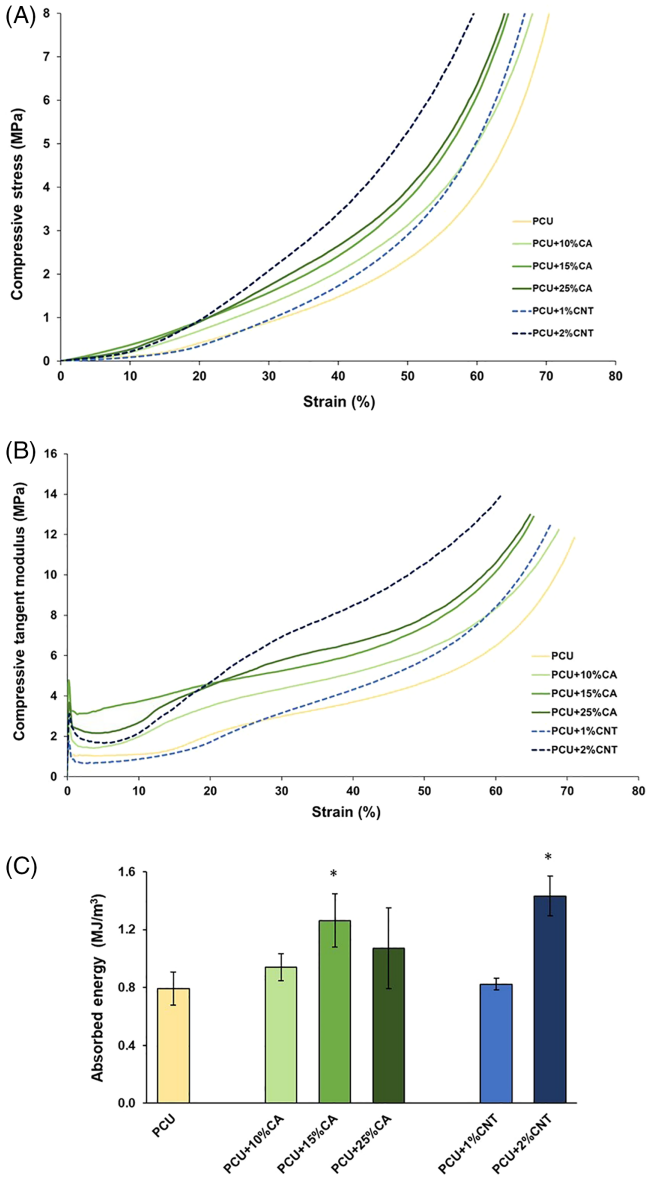

FIGURE 3 Mechanical properties of PCU-based materials obtained from compression tests. (A) Compressive stress–strain curves; (B) Compressive tangent modulus calculated in the 0%–60% strain range; (C) Absorbed energy until a deformation of 60%. The symbol * identifies statistically significant differences relative to PCU. The error bars correspond to ± SD

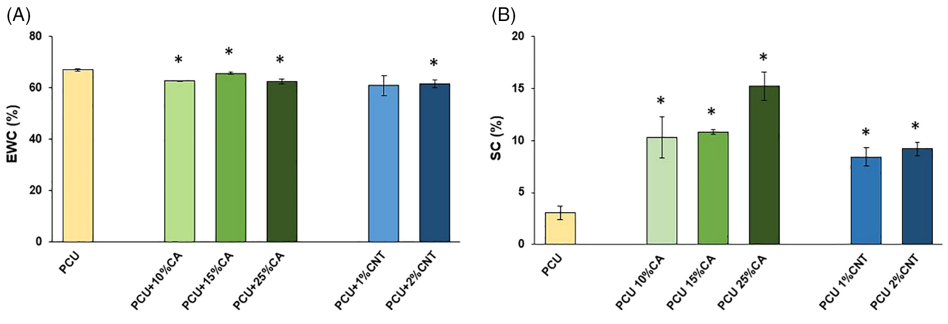

FIGURE 2 (A) Equilibrium water content (%EWC) of the as-produced materials and (B) swelling capacity (% SC) of the materials after being dried. The symbol * identifies statistically significant differences relative to PCU. The error bars correspond to ±SD

were applied to compare three or more and two independent groups, respectively. The level of significance chosen was .05.

3 | RESULTS

3.1 | Equilibrium water content and swelling capacity

Figure 2A presents the equilibrium water content of the materials as-produced. Although, from the statistical point of view, differences had been observed ($p < .03$), the average values were quite similar, ranging between 62% and 67%. Figure 2B shows the swelling capacity of the materials after being dried. PCU presents the lowest value (3%), while the remaining materials have values close to 10%, except PCU + 25% CA, which shows ≈ 15%.

3.2 | Mechanical properties

3.2.1 | Compressive tests

The stress–strain curves obtained in the compression tests performed with the different hydrogels are depicted in Figure 3.

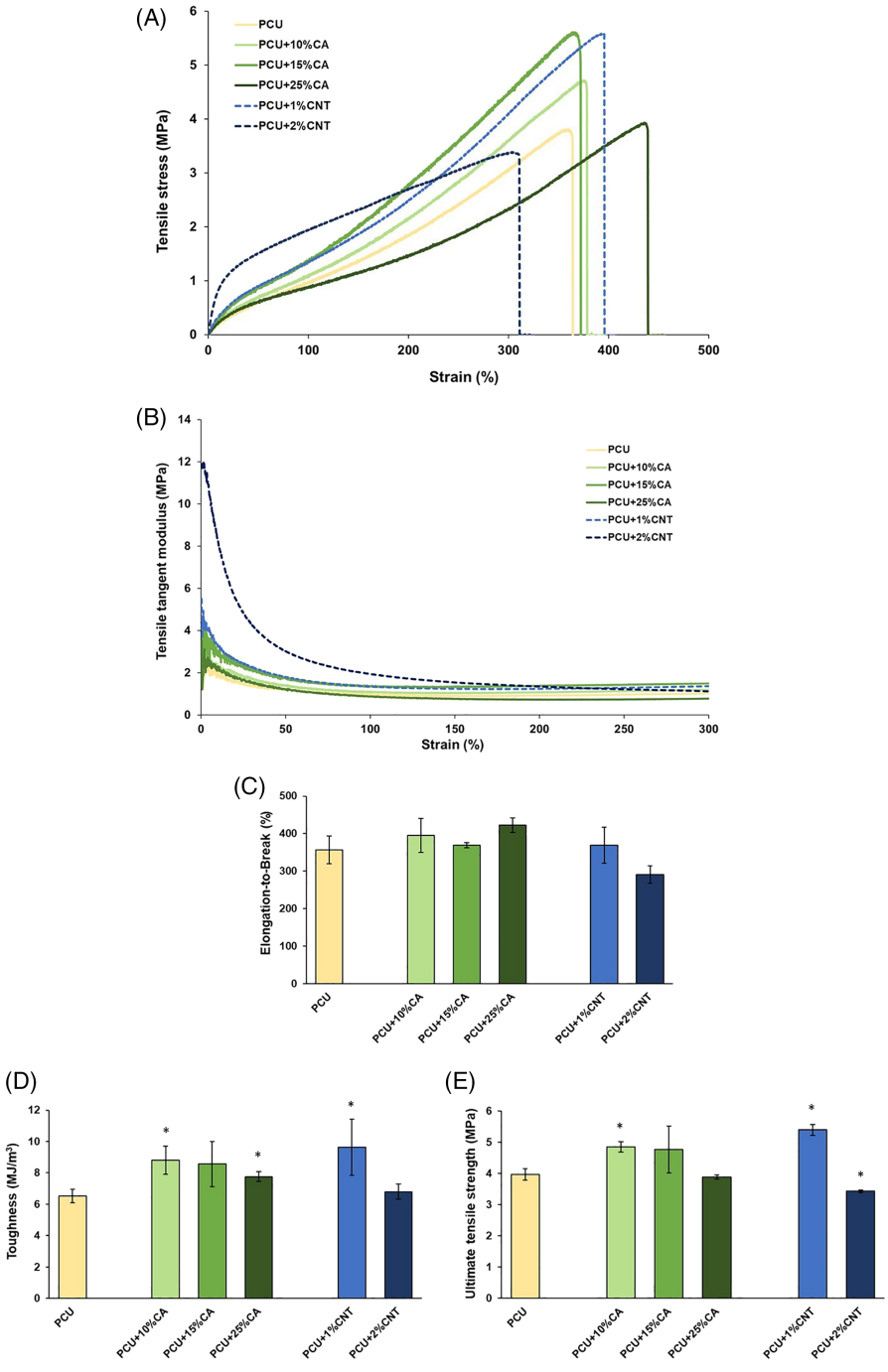

FIGURE 4 Mechanical properties of PCU-based materials obtained from tensile tests. (A) Tensile stress–strain curves; (B) Tensile tangent modulus calculated in the 0%–300% strain range, (C) Elongation-to-break; (D) Toughness and (E) Ultimate tensile strength. The symbol * identifies statistically significant differences relative to PCU. The error bars correspond to ± SD

The variation of the compressive tangent modulus along the experiments, as well as the absorbed energy during the compression estimated from these curves, are also shown. The addition of CA at a percentage ≥ 15% or of CNT at 2% led to materials with the highest mechanical resistance (Figure 3A). Regarding the tangent modulus (Figure 3B), the addition of CA led to a significant increase in the whole strain range. Above 20% strain, the modulus becomes similar for concentrations > 15%. As for CNT, while 1% reinforcement almost did not change the modulus values relative to PCU (except for high strains), 2% resulted in the highest modulus among the studied hydrogels. The absorbed energy values till a deformation of 60% are shown in Figure 3C (see also Table S1 in Supplementary Information). The highest values were obtained for PCU + 15%CA and PCU + 2%CNT ($p < .003$).

3.2.2 | Tensile tests

The stress–strain curves obtained for the tensile tests are shown in Figure 4A. The mechanical behavior of the hydrogels depends on the nature and concentration of the reinforcement agent. The curve shape was different in the case of PCU + 2%CNT. This material stands out due to its much superior tensile tangent modulus for strains under 130% (Figure 4B). The elongation-to-break average values did not present statistically significant differences for the studied hydrogels ($p > .08$, Figure 4C and Table S1 in Supplementary Information). Both the addition of CA and CNT improved the materials' toughness (Figure 4D and Table S1 in Supplementary Information): 19%–35% in the former case, while CNTs led to an increase of 4%–48%, being the highest value observed for PCU + 1%CNT.

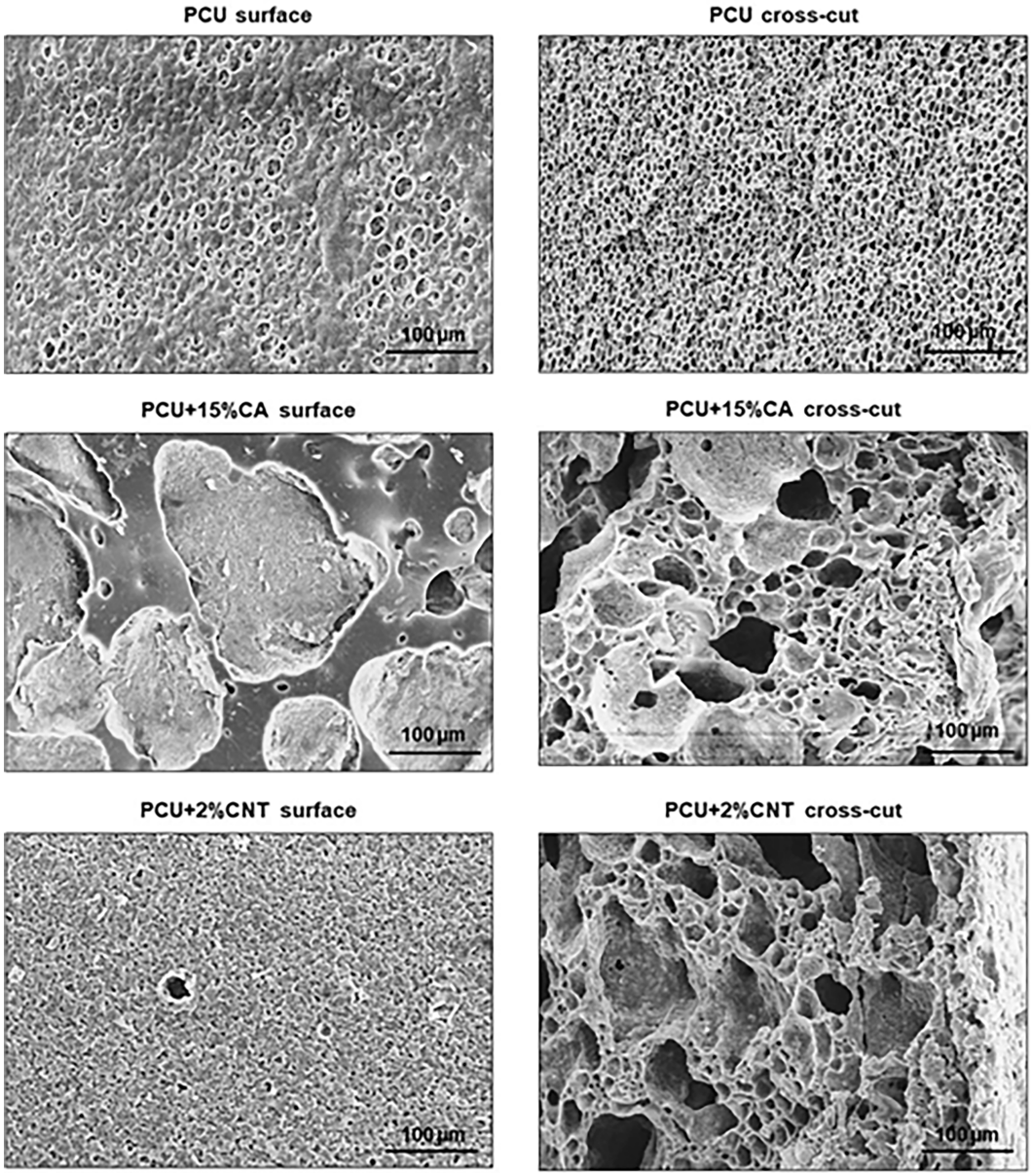

FIGURE 5 Scanning electron microscope (SEM) images of the surface and cross-cut of PCU, PCU + 15%CA, and PCU + 2%CNT

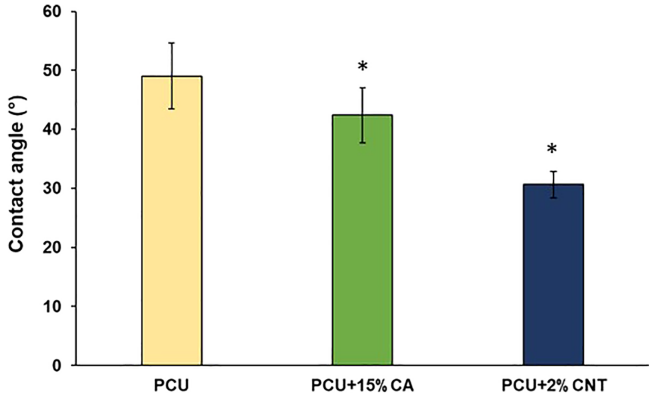

FIGURE 6 Water contact angles with PCU, PCU + 15%CA, and PCU + 2%CNT. The symbol * identifies statistically significant differences relative to PCU. The error bars correspond to ± SD

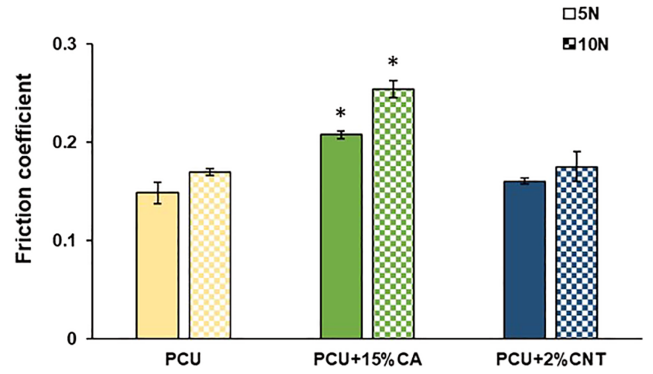

FIGURE 7 Friction coefficient of PCU, PCU + 15%CA, and PCU + 2%CNT measured against SS 316 L using PBS + HA solution as lubricant. The symbol * identifies statistically significant differences relative to PCU. The error bars correspond to ± SD

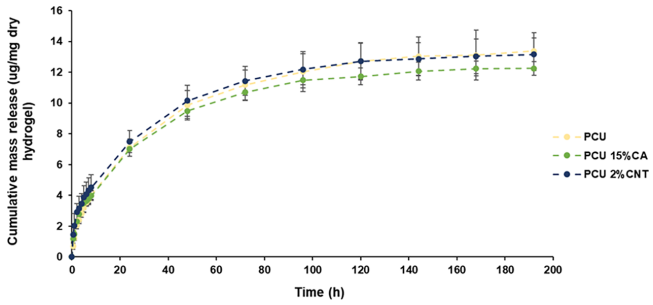

FIGURE 8 Cumulative drug release profiles of DFN from PCU, PCU + 15%CA, and PCU + 2%CNT. The error bars correspond to ± SD

Concerning the ultimate tensile strength, the average values also increased except for the highest concentrations of the reinforcements (Figure 4E and Table S1 in Supplementary Information).

Since cartilage replacement materials' compressive behavior is more relevant for their in vivo performance, PCU + 15%CA and PCU + 2%CNT were considered the best performing materials and selected for further characterization.

TABLE 2 Amounts of drug loaded and percentage of drug released for the different materials

	Amount of drug loaded (μg/mg dry hydrogel)	% Drug released
PCU	0.74 ± 0.16	79.2 ± 3.3
PCU + 15%CA	0.65 ± 0.05	83.7 ± 1.6
PCU + 2%CNT	0.64 ± 0.08	83.6 ± 3.0

3.3 | Morphology

The microstructure of the studied materials is depicted in Figure 5. It can be observed that PCU presents a porous structure both on its surface and in the cross-cut. The addition of 15% CA led to an increase of heterogeneity with the appearance of pores of distinct sizes. PCU + 2%CNT shows fewer pores on the surface and a particular irregular cross-cut area.

3.4 | Wettability

The contact angle results for PCU, PCU + 15%CA, and PCU + 2% CNT are depicted in Figure 6. It can be observed that all materials are hydrophilic, being the contact angle for PCU + 15%CA and PCU + 2%CNT significantly lower than for PCU ($p = .01$ and $p < .001$, respectively). PCU + 2%CNT shows the highest reduction.

3.5 | Friction coefficient

The CoF results are presented in Figure 7. CoF values change with the applied load: the higher the load, the higher the CoF. PCU + 15%CA presents a higher CoF than PCU both for 5 N ($p = .003$) and 10 N ($p < .001$). PCU + 2%CNT present similar values to PCU ($p > .2$).

3.6 | Drug release

The cumulative DFN release profiles from PCU, PCU + 15%CA, and PCU + 2%CNT samples are shown in Figure 8. The drug release profiles are quite similar, although PCU + 15%CA had led to a slightly lower amount of drug released. The materials ensured a sustained release during more than 4 days (96 h), being observed a decrease in the drug release rate along the time.

The amount of drug loaded into each material as well the corresponding percentage of drug released at the end of the experiment are presented in Table 2. The amount of drug loaded by PCU was slightly higher than that observed for the reinforced materials. However, the difference is not statistically significant ($p = .174$). Concerning the percentage of drug released relative to the total amount of drug loaded, although PCU has led to a slightly lower value than

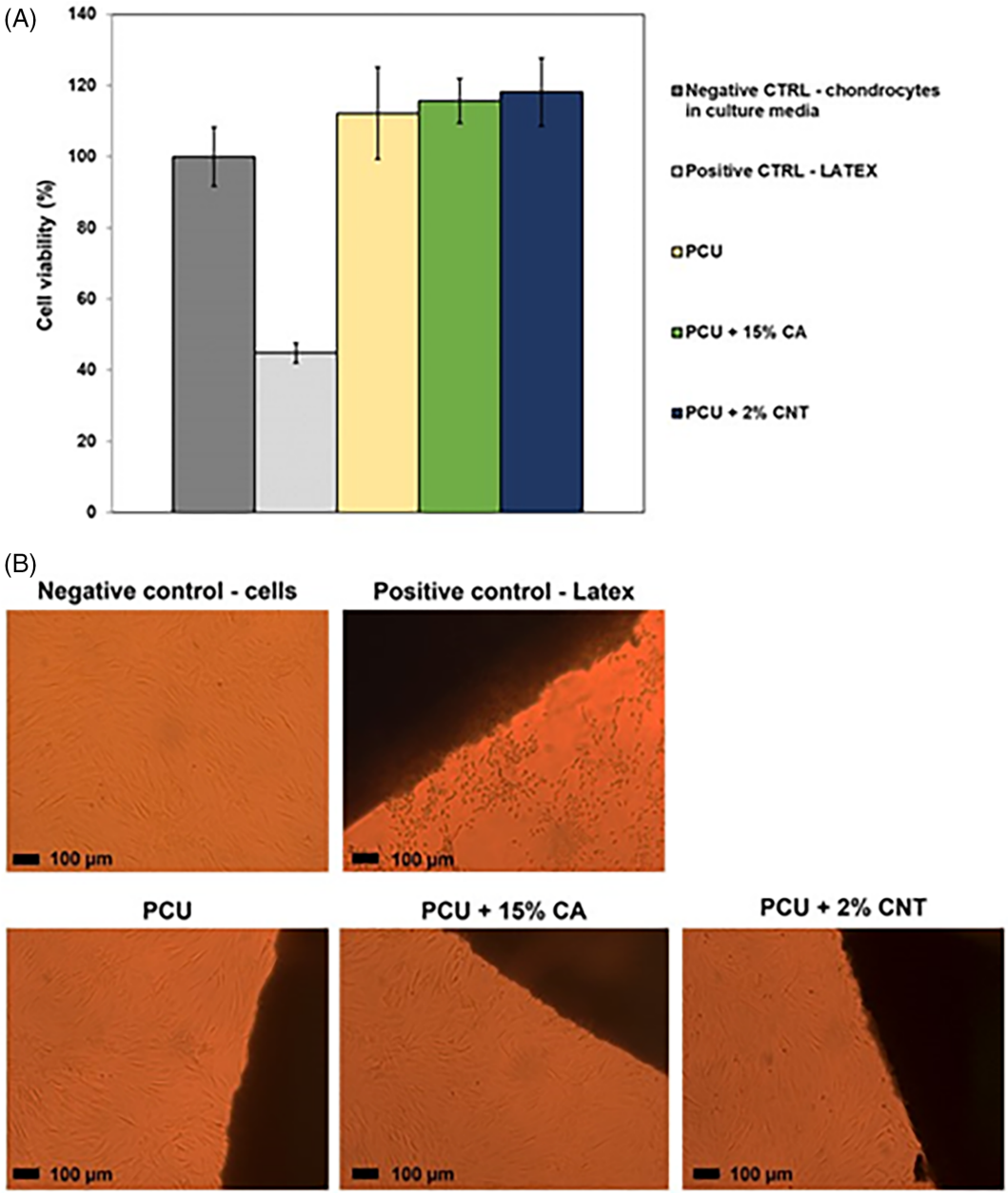

FIGURE 9 (A) Percentage of viable cells determined through MTT indirect tests for PCU, PCU + 15%CA, and PCU + 2%CNT and respective negative/positive controls and (B) Chondrocyte morphology observed by optical microscopy in the direct contact tests

PCU + 15%CA and PCU + 2%CNT, again, the differences are not significant ($p = .073$).

3.7 | Cytotoxicity evaluation

Cytotoxicity tests were carried out with PCU, PCU + 15%CA, and PCU + 2%CNT samples. The MTT indirect test showed that chondrocytes cultured with extract conditioned medium for 48 h presented in all cases high cell viability (≈ 100%, Figure 9A) in relation to the negative control. In addition, cells cultured in direct contact with the materials for 48 h showed typical chondrocyte morphology with no evidence of cell death and any inhibition halo effect (Figure 9B).

4 | DISCUSSION

In this work, PCU-based hydrogels intended for articular cartilage replacement were developed. Different amounts of CA and CNT were incorporated as reinforcements to improve the material's properties. Their equilibrium water content and compressive and tensile mechanical behavior were accessed. The materials that revealed the most promising properties were selected and characterized in terms of

morphology, wettability, and CoF. Besides, DFN was loaded in the hydrogels, and drug release profiles were obtained. Finally, the material that showed the best drug release behavior was submitted to cytotoxicity tests to investigate its biocompatibility.

PUs are segmented copolymers constituted by a soft segment (a polyester, a polyether, or a polycarbonate) and hard segments (a diisocyanate and chain extender).[50] Polyester urethanes suffer fast hydrolytic degradation of the aliphatic polyester soft segment, which turns them into unsuitable materials to be used in long-term implantation devices. Contrarily, polyether urethanes present high hydrolytic stability, but they undergo oxidative degradation, namely environmental stress cracking and metal ion oxidation[51–53] PCUs reveal a superior performance since they allow to minimize cracking or degradation upon implantation for a long period of time,.[54] PCU usually gives rise to hydrophobic materials (water contact angle >100°[55] with low water uptake capacity (1.2%–2.1%).[56] In this work, PCU was used to produce hydrogels for cartilage replacement. As far as the authors know, this was the first time that PCU hydrogels were produced. PCU was dissolved in a mixture of acetone and DMF which was poured into a petri dish and left in open air for 24 h. This resulted in an increase of the polymer concentration due to the partial evaporation of the solvents (mainly acetone, due to its higher volatility). Thereafter, the plate was immersed in water (nonsolvent) to coagulate the solution by exchanging the solvents. The immersion of the homogeneous polymer solution in the water coagulation bath leads to the formation of two phases: a polymer-rich phase and a liquid-rich phase.[57] The solvent diffuses through the nonsolvent and the nonsolvent through the polymer solution. The concentration of the polymer, the nature of the solvent and nonsolvent, the time of precipitation and the temperature of the bath, may significantly affect the morphology and properties of the obtained material (e.g., porosity, mechanical behavior). If the material is not dried, it will have a high content of water, presenting a hydrogel-like behavior. Such high water content usually leads to low mechanical properties. In order to improve the material's tribomechanical performance, they were reinforced with CA and carbon nanotubes (CNT).

The addition of CA and CNT almost did not affect the equilibrium water content of the PCU hydrogels. The obtained values are close to the range found in the literature for the articular cartilage, which is 65–80% of its wet weight.[58] In order to evaluate the reversibility of the swelling process after drying, dried samples were immersed in water and left equilibrate. The swelling capacity (%SC) was determined and it was found that with exception of PCU, which led to a % SC of 3%, all the other materials present %SC close to 10% or higher. The highest value was observed for PCU + 25%CA (≈15%) and may be explained by the hydrophilic nature of CA reinforcement and/or differences in porosity. During the drying process, water evaporates leading to the structure collapse and to shrinking of the material. When immersed in water, the materials only were able to absorb a limited amount of water compared to the initial one, showing the hydration process is only barely reversible. There is no lower limit to define how much water a material has to absorb to be called a hydrogel.[59] The amount of water can vary considerably, from 10% up to a thousand times of their dry weight.[60,61] Therefore, all materials, except PCU can be classified as hydrogels. Since the produced materials are intended to be used for cartilage substitution, it is desirable that they present properties as similar as possible to articular cartilage tissue. For this reason, in the following characterization tests, we opted by proceeding with the materials as-produced (without drying).

Regarding the materials' compressive mechanical properties, the stress–strain curves follow a typical behavior of hydrogels. Since the hydrogel is a biphasic material, at the beginning of the compression tests, the applied load is supported essentially by the fluid phase. With the increase in the load, the fluid begins to exit the matrix, and load is transferred from the fluid to the solid phase. The curves' analysis shows that in the first stages of compression (till ≈ 1 MPa), the addition of 1% of CNT to PCU does not affect the mechanical behavior of the hydrogel (Figure 3A). For higher stresses, there is a visible increase of resistance to deformation of PCU + 1%CNT: the compressive tangent modulus increases for the reinforced material (Figure 3B), indicating that it is stiffer than the original material. The addition of 2% CNT led to an initial decrease in the tangent modulus, which can be attributed to the water exit that shall interact less with the polymeric matrix due to the presence of the CNTs. Above 10% strain, the resistance to deformation of PCU + 2%CNT increases significantly (the modulus increases) due to the solid phase response. The improvement in tangent modulus can be attributed to the load transfer from the polymeric matrix to the CNTs, which present a high elastic modulus (400 GPa-4.15 TPa[62]). Such reinforcement resulted in a material able to absorb a higher amount of energy among the studied hydrogels. Regarding CA incorporation, it also led to an improvement of the PCU performance at compression, with a significant increase in the tangent modulus. It is observed that for 15% CA, until 40% strain, the modulus increases almost linearly, which suggests that the fluid phase does not affect the compressive behavior of the hydrogel. Bellow and above this content in CA a decrease in the tangent modulus is observed in the initial stages of compression which should be related to the outflow of water, as referred above. For higher strains, the mechanical behavior of the reinforced materials with ≥15% CA becomes similar. PCU + 15%CA presented the highest capacity of energy absorption. The improvement resultant from CA addition may be attributed to the formation of hydrogen bonds between the N—H groups from urethane carbonate and C═O groups of CA. Both CNT and CA reinforcements led to tangent modulus values that, although varying with strain, are of the same order of magnitude of those found in the literature for human articular cartilage (0.24–10 MPa).[63–65] Comparison of the values obtained for the absorbed energy is more difficult since it depends on the limits defined for its calculation (e.g., stress, percentage strain) and testing parameters.

Concerning the tensile behavior, it was observed that the addition of both CA and CNT reinforcements led, in general, to the improvement of the mechanical behavior of all hydrogels, except PCU + 25% CA. There is a notorious difference between the PCU + 2%CNT and the other reinforced hydrogels (Figure 4A). Until 1 MPa, there is a fast increase of the strength behavior that shall result from the mechanical anchorage provided by the CNTs. However, for higher applied loads,

an inflection of the curve is observed, suggesting a decrease of the support action of the CNTs, which shall be due to the loss of adhesion of the reinforcement with the matrix. For a deformation until ≈25%, the tangent modulus is between 5 and 12 MPa (Figure 4B), which falls in the range of the values found for human articular cartilage (5–25 MPa).[66] In respect of the ultimate tensile strength, both for CA and CNTs, a decrease was noticed after a threshold of the reinforcement content, which according to Huang et al.[67] results from the dispersion heterogeneity that shall occur for higher concentrations. Values found in the literature for the ultimate tensile strength of articular cartilage range between 9 and 40 MPa, while elongation-at-break presents values within 60–120%. These values are somehow different from those observed for the studied materials, but as mentioned before, tensile properties are less relevant for the in vivo performance of the materials than the compressive ones.

The reinforcement effect of both CNTs and CA agrees with what was observed by other authors for different polymers. Tong et al.[40] and *Huang* et al.[67] reinforced PVA with different contents of CNTs and found an increase of the tensile modulus, tensile strength, and elongation-to-break. In turn, Knapczyk-Korczak et al.[68] found that the addition of CA to polystyrene led to a more durable and mechanically stable material. Also, Kurokawa et al.[69] observed that the mechanical properties of polylactic acid were improved by CA addition. Tang et al.[38] fabricated CA/PU composite nanofibers with different concentrations of CA and observed that 20% of CA led to the best tensile performance.

PCU + 15%CA and PCU + 2%CNT present the most encouraging mechanical properties for each type of reinforcement, and therefore they were chosen for further characterization. In fact, PCU + 15%CA led to the highest compressive (until 20%) and tensile tangent modulus. In turn, PCU + 2%CNT showed superior mechanical resistance at compression and the highest tensile resistance until a deformation of 130% and tensile tangent modulus.

The morphology of the materials was studied by SEM. It was observed that both PCU and the reinforced materials PCU + 15%CA and PCU + 2%CNT have a porous structure (Figure 5). The porosity of the materials may be strongly affected by the preparation conditions, namely the solvent exchange. In fact, according to Lee et al.,[70] the combination of two different solvents shall lead to a higher porosity compared to the use of one unique solvent. Apart from the surface tension of the exchanged solvents, the affinity between the solvents and the polymer, structural changes induced during the solvents exchange, and the shrinkage that occurs during the solvent exchange and drying contribute to the increased porosity. The addition of CA led to significant changes in the materials' morphology. The pores size and respective size distribution increased. Contrarily, the presence of CNTs turned the surface more compact, although the interior part remained porous but with high heterogeneity. The addition of reinforcement agents may significantly change the porosity of the materials. Several factors may affect such characteristic, for example, the chemical nature, the particle size and shape, and the amount of reinforcement, being difficult to predict the result of the reinforcement addition. The increased heterogeneity in the pore size distribution observed for PCU + 15%CA and PCU + 2%CNT may also be related to difficulties in dispersing the strengthening agents. Although for CA reinforced materials, no data were found in literature concerning its effect on porosity, for CNTs, several authors report significant changes, depending on the hydrogel nature and its interaction with the CNTs.[39,71] Lan et al.[72] observed a decrease of porosity of polyvinyl alcohol/biphasic calcium phosphate hydrogels till a certain content of CNTs. Also, Chen et al.[71] found a decrease in the number of pores with CNTs' addition and related it to the CNTs hydrophobic nature and their ability to displace the hydrophilic components of the hydrogel network, decreasing its density.

Both the addition of CA and CNTs improved the PCU hydrophilicity. CA presents a hydrophilic nature due to the hydroxyl groups, which can explain the decrease in the water contact angle.[73] Contrarily, CNTs are generally recognized by their hydrophobicity and usually form insoluble aggregates.[74] According to Wang et al.,[75] the presence of DMF is critical to minimize CNTs agglomeration because the methyl groups are adsorbed on the CNTs, while the amine groups attract the water molecules due to their high polarity. On the other hand, Manorma et al.[76] observed a reduction in the contact angle in polysulfone nanofiltration membranes when CNTs were added, which they attributed to a reduction of roughness. Thus, the nanotubes' surface functionalization due to the action of DMF and the decrease of the surface roughness, which is associated with the porosity decrease, shall explain the observed reduction of the contact angle.

Since these materials are expected to be used as replacements for articular cartilage, the assessment of the CoF is very important. Indeed, a higher CoF usually leads to a higher effort by the patient in the joint movement. For all tested materials, it was found an increase of the average CoF with the applied load. This may be related to the increase of the contact area, leading to a rise of the adhesion forces and the penetration depth of the counterbody into the hydrogel. During reciprocating sliding, the hydrogel is submitted to compression and tensile stress fields, leading to squeezing and swelling cycles of the liquid, which shall influence the surface lubrication. The increased amount of lubricant in the interfacial zone, due to the hydrogel's squeezing, is expected to reduce the CoF. The higher compressive tangent modulus of PCU + 15%CA (Figure 3B) shall turn the release of water from the matrix more difficult than for PCU and PCU + 2% CNT. Also, PCU + 15%CA presents a higher porosity which might increase roughness and friction (Figure 5).

As previously referred, hydrogels may be used as platforms for drug delivery. In this work, the potential of PCU + 15%CA and PCU + 2%CNT to elute an anti-inflammatory, diclofenac, after cartilage repair surgery was evaluated and compared to bare PCU. Since it was observed that the dry materials have a low swelling capacity (Figure 2B), the materials were loaded by soaking the hydrated samples in a DFN solution. This shall allow a higher amount of drug loaded, as an easier diffusion of the drug will occur into the material. The drug release results (Figure 8 and Table 2) show that the addition of both CNTs and CA did not significantly impact the amount of drug loaded, as well as the percentage of drug released and drug release profiles, when compared to PCU. All materials ensured a controlled

release for at least 4 days. It was expected that DFN sodium, due to its hydrophilic nature,[77] had a higher affinity for the materials containing hydrophilic CA, which is also hydrophilic. Although a slight reduction was found in the amount of drug released (Figure 8), which could mean a stronger interaction, this was not statistically significant. Other authors reached similar conclusions: Adepu et al.,[78] studied the release of diclofenac sodium from electrospun CA nanofibers and found that this drug does not establish any chemical interaction with CA. Infra-red spectroscopy analysis suggested the formation of hydrogen bonding between the drug and the CA fibers. In order to infer about the mechanism of drug transport, the release profiles were fitted to the Korsmeyer-Peppas equation[79]:

$$\frac{M_t}{M_\infty} = Kt^n \quad (3)$$

where M_t and M_∞ are the masses released at time t and as the time approaches infinity, respectively, n is the diffusional exponent and K is the pseudo-kinetic constant. Table Curve 2D, v5 was used to determine the M_∞ and to fit the experimental values until the first 60% of the fractional release. The correlation coefficients (R^2) are ≥ 0.988 in all cases showing that the model is suitable to describe the drug release behavior. More, the values of n are close to 0.5 (0.527 for PCU, 0.454 for PCU + 15%CA, and 0.415 for PCU + 2%CNT), indicating a Fickian or pseudo-Fickian behavior with a diffusion-controlled mechanism.[79,80]

Finally, the cytotoxicity of PCU, PCU + 15%CA, and PCU + 2% CNT was studied. The results demonstrate that the materials do not induce any harmful effect on human chondrocytes viability and morphology, which is in accordance with previous studies reporting the use of these materials individually to fabricate scaffolds for different tissue regeneration applications.[81,82] Moreover, Shrestha et al.[83] showed that electrospun CA-based nanofibrous scaffolds were biocompatible for the growth of primary chondrocytes.

5 | CONCLUSIONS

In this work, the possibility of producing PCU hydrogels for cartilage replacement loaded with diclofenac was investigated. The materials were reinforced with different amounts of CA (10%, 15%, and 25% w/w) or carbon nanotubes (CNTs, 1% and 2% w/w). The results showed that the addition of the reinforcements almost did not change the equilibrium water content of PCU hydrogel, which remained within the values found for natural human cartilage. The best mechanical properties were found for PCU + 15%CA and PCU + 2%CNT. Therefore, these materials were chosen for further characterization, being compared to nonreinforced PCU.

Regarding morphology, the addition of 15% CA significantly increased the porosity, while 2% CNT led to the opposite effect. The hydrophilicity of the materials slightly increased for both reinforcements. The CoF value in measurements against stainless steel 316 L was not affected by the addition of CNTs. Contrarily, a slight increase was observed when CA was present, but the values remained of the same order of magnitude, being lower than 0.25. The materials were loaded by soaking with diclofenac, aiming to obtain drug delivery devices that can help to minimize the postsurgical inflammatory reactions. The materials led to similar release profiles, being able to ensure a controlled release of the anti-inflammatory for at least 4 days. Although the therapeutic efficacy of the system only could be truly accessed through in vivo systems, it shall be stressed that it can be improved by adjusting the drug-loading concentrations to obtain higher amounts of drug released. Finally, cytotoxicity tests carried out with chondrocytes showed that none of the materials impaired cell viability.

As far as the authors know, this was the first time that PCU hydrogels were produced. Drug loaded materials intended for articular cartilage replacement were developed, but other applications may be foreseen. Further studies will be needed to better characterize the material's behavior and tune its properties for each specific application.

ACKNOWLEDGMENTS

To Fundação para a Ciência e a Tecnologia (FCT) for funding through the project CartHeal - PTDC/CTM-CTM/29593/2017 and the unit projects UIDB/00100/2020, UIDB/04585/2020, UID/CTM/04540/2020 and UIDB/50022/2020 (LAETA) from CQE, CiiEM, CeFEMA and IDMEC respectively, and for the PhD grants of A.S Oliveira (PD/BD/128140/2016) and A.C. Branco (SFRH/BD/145423/2019).

CONFLICTS OF INTEREST

The authors declare no conflict of interest.

DATA AVAILABILITY STATEMENT

The data that support the findings of this study are available from the corresponding author, Ana Paula Serro, upon reasonable request.

ORCID

Ana C. Branco https://orcid.org/0000-0003-2773-6475
Diana Silva https://orcid.org/0000-0003-0102-7048
Ana P. Serro https://orcid.org/0000-0002-6179-9296

REFERENCES

1. Castañeda S, Vicente EF. Osteoarthritis: more than cartilage degeneration. Clin rev bone miner Metab. Clinical reviews in bone and mineral. *Metabolism*. 2017;15:69-81.
2. Loeser RF, Goldring SR, Scanzello CR, Goldring MB. Osteoarthritis: a disease of the joint as an organ. *Arthritis Rheum*. 2012;64:1697-1707.
3. Räsänen P, Paavolainen P, Sintonen H, et al. Effectiveness of hip or knee replacement surgery in terms of quality-adjusted life years and costs. *Acta Orthop*. 2007;78:108-115.
4. De l'Escalopier N, Anract P, Biau D. Surgical treatments for osteoarthritis. *Ann Phys Rehabil Med*. 2016;59:227-233.
5. Merola M, Affatato S. Materials for hip prostheses: a review of wear and loading considerations. *Materials (Basel)*. 2019;12:1-24.
6. Hu CY, Yoon TR. Recent updates for biomaterials used in total hip arthroplasty. *Biomater Res*. 2018;22:1-12.
7. Windler M, Klabunde R. Titanium for hip and knee prostheses. *Titan Med*. 2001;1:703-746.

8. Hussain O, Saleem S, Ahmad B. Implant materials for knee and hip joint replacement: a review from the tribological perspective. *Mater Sci Eng*. 2019;561:1-7.
9. Sumner DR. Long-term implant fixation and stress-shielding in total hip replacement. *J Biomech*. 2015;48:797-800.
10. Ren K, Dusad A, Zhang Y, Wang D. Therapeutic intervention for wear debris-induced aseptic implant loosening. *Acta Pharm Sin B*. 2013;3:76-85.
11. Figueiredo-Pina CG, Dearnley PA, Fisher J. UHMWPE wear response to apposing nitrogen S-phase coated and uncoated orthopaedic implant grade stainless steel. *Wear*. 2009;267:743-752.
12. Jorgensen AM, Edgar CM, Geaney LE, Talar M. Talar Osteochondral Autograft Transplant. *Tech Foot Ankle Surg*. 2020;19:190-196.
13. Li J, Mooney DJ. Designing hydrogels for controlled drug delivery. *Nat Rev Mater*. 2016;1:1-18.
14. Oinas J, Ronkainen AP, Rieppo L, et al. Composition, structure and tensile biomechanical properties of equine articular cartilage during growth and maturation. *Sci Rep*. 2018;8:1-12.
15. Vigata M, Meinert C, Hutmacher DW, Bock N. Hydrogels as drug delivery systems: a review of current characterization and evaluation techniques. *Pharmaceutics*. 2020;12:1-45.
16. Saghazadeh S, Rinoldi C, Schot M, et al. 1Biomaterials. Drug delivery systems and materials for wound healing applications. *Adv Drug Deliv Rev*. 2018;127:138-166.
17. Aguilar Z. Targeted drug delivery (chapter 5). *Nanomaterials for Medical Applications*. 2013;1:181-234.
18. Diclofenac epolamine Monograph for Professionals. 2018 https://www.drugs.com/monograph/diclofenac-systemic.html
19. Mcloughlin C, Mckinney MS, Fee JPH, Boules Z. Diclofenac for day-care arthroscopy surgery: comparison with a standard opioid therapy. *Br J Anaesth*. 1990;65:620-623.
20. Oliveira AS, Seidi O, Ribeiro N, Colaço R, Serro AP. Tribomechanical comparison between PVA hydrogels obtained using different processing conditions and human cartilage. *Materials (Basel)*. 2019;12:3413.
21. Oliveira AS, Schweizer S, Nolasco P, et al. Tough and low friction polyvinyl alcohol hydrogels loaded with anti-inflammatories for cartilage replacement. *Lubricants*. 2020;8:1-22.
22. Rey-Rico A, Madry H, Cucchiarini M. Hydrogel-based controlled delivery Systems for Articular Cartilage Repair. *Biomed Res Int*. 2016;2016:1-12.
23. Inyang AO, Vaughan CL. Functional characteristics and mechanical performance of PCU composites for knee meniscus replacement. *Materials (Basel)*. 2020;13:1-16.
24. Elsner JJ, McKeon BP. Orthopedic application of polycarbonate urethanes: a review. *Tech Orthop*. 2017;32:132-140.
25. Christenson EM, Dadsetan M, Wiggins M, Anderson JM, Hiltner A. Poly(carbonate urethane) and poly(ether urethane) biodegradation: in vivo studies. *J Biomed Mater Res - Part A*. 2004;69:407-416.
26. Majd SE, Rizqy AI, Kaper HJ, Schmidt TA, Kuijer R, Sharma PK. An in vitro study of cartilage–meniscus tribology to understand the changes caused by a meniscus implant. *Colloids Surfaces B Biointerfaces*. 2017;155:294-303.
27. Kanca Y, Milner P, Dini D, Amis AA. Tribological evaluation of biomedical polycarbonate urethanes against articular cartilage. *J Mech Behav Biomed Mater*. 2018;82:394-402.
28. Elsner JJ, Portnoy S, Zur G, Guilak F, Shterling A, Linder-Ganz E. Design of a free-floating polycarbonate-urethane meniscal implant using finite element modeling and experimental validation. *J Biomech Eng*. 2010;132:1-8.
29. Linder-ganz E, Elsner JJ, Zur G, et al. Chondroprotective effects of a polycarbonate-urethane meniscal implant: semi-quantitative results in a sheep model. *Proc ASME 2010 Summer Bioeng Conf*. 2016;19:6-7.
30. Abar B, Alonso-Calleja A, Kelly A, Kelly C, Gall K, West JL. 3D printing of high-strength, porous, elastomeric structures to promote tissue integration of implants. *J Biomed Mater Res - Part A*. 2021;109:54-63.
31. Beckett LE, Lewis JT, Tonge TK, Korley LSTJ. Enhancement of the mechanical properties of hydrogels with continuous fibrous reinforcement. *ACS Biomater Sci Eng*. 2020;6:5453-5473.
32. Utech S, Boccaccini AR. A review of hydrogel-based composites for biomedical applications: enhancement of hydrogel properties by addition of rigid inorganic fillers. *J Mater Sci. Springer US*. 2016;51:271-310.
33. Mustapha S, Andou Y. Enhancing mechanical properties of polyurethane with cellulose acetate as chain extender. *Fibers Polym*. 2021;22:2112-2118.
34. Salama A, Mohamed A, Aboamera NM, Osman T, Khattab A. Characterization and mechanical properties of cellulose acetate/carbon nanotube composite nanofibers. *Adv Polym Technol*. 2018;37:2446-2451.
35. Kaur G, Grewal J, Yoti K, Jain U, Chandra R, Madan J. Oral controlled and sustained drug delivery systems: concepts, advances, preclinical, and clinical status. *Drug Target Stimuli Sensitive Drug Deliv Syst*; 2018;1:567-626. Elsevier Inc.
36. Girouard NM, Xu S, Schueneman GT, Shofner ML, Meredith JC. Site-selective modification of cellulose nanocrystals with Isophorone Diisocyanate and formation of polyurethane-CNC composites. *ACS Appl Mater Interfaces*. 2016;8:1458-1467.
37. Yuwawech K, Wootthikanokkhan J, Wanwong S, Tanpichai S. Polyurethane/esterified cellulose nanocrystal composites as a transparent moisture barrier coating for encapsulation of dye sensitized solar cells. *J Appl Polym Sci*. 2017;134:1-12.
38. Tang C, Chen P, Liu H. Cocontinuous cellulose acetate/ polyurethane composite nanofiber fabricated through electrospinning. *Polym Eng Sci*. 2008;48:1296-1303.
39. Mihajlovic M, Mihajlovic M, Dankers PYW, Masereeuw R, Sijbesma RP. Carbon nanotube reinforced supramolecular hydrogels for bioapplications. *Macromol Biosci*. 2019;19:1-12.
40. Tong X, Zheng J, Lu Y, Zhang Z, Cheng H. Swelling and mechanical behaviors of carbon nanotube/poly(vinyl alcohol) hybrid hydrogels. *Mater Lett*. 2007;61:1704-1706.
41. Saito N, Usui Y, Aoki K, et al. Carbon nanotubes for biomaterials in contact with bone. *Curr Med Chem*. 2008;15:523-527.
42. Anzar N, Hasan R, Tyagi M, Yadav N, Narang J. Carbon nanotube - a review on synthesis, properties and plethora of applications in the field of biomedical science. *Sensors Int*. 2020;1:100003.
43. Wang W, Zhu Y, Liao S, Li J. Carbon nanotubes reinforced composites for biomedical applications. *Biomed Res Int*. 2014;2014:1-14.
44. Xia H, Song M. Preparation and characterization of polyurethane-carbon nanotube composites. *Soft Matter*. 2005;1:386-394.
45. Khang D, Park GE, Webster TJ. Enhanced chondrocyte densities on carbon nanotube composites: the combined role of nanosurface roughness and electrical stimulation. *J Biomed Mater Res - Part A*. 2008;86:253-260.
46. Bass RW Synthesis and characterization of self-healing poly (carbonate urethane) carbon-nanotube. Doctoral Dissertation, University of South Florida,Tampa, USA, 2011
47. Bodenberger N, Kubiczek D, Abrosimova I, et al. Evaluation of methods for pore generation and their influence on physio-chemical properties of a protein based hydrogel. *Biotechnol Reports*. 2016;12:6-12.
48. Inoue TOH. Drying method of biological specimens for scanning method microscopy: the t-butyl alcohol. *Arch Histol Cytol*. 1988;51:53-59.
49. International Organization for Standardization. *Biological Evaluation of Medical Devices—Part 5 Tests for Citotoxicity (ISO EN 10993–5) and Part 12: Sample Preparation and Reference Materials (ISO EN 10993–12)*. 2012. ISO.
50. Jiang L, Ren Z, Zhao W, Liu W, Liu H, Zhu C. Synthesis and structure/properties characterizations of four polyurethane model hard segments. *R Soc Open Sci*. 2018;5:1-11.
51. Stokes K, Mcvenes R, Anderson JM. Polyurethane elastomer biostability. *J Biomater Appl*. 1995;9:321-354.

52. Wiggins MJ, Wilkoff B, Anderson JM, Hiltner A. Biodegradation of polyether polyurethane inner insulation in bipolar pacemaker leads. *J Biomed Mater Res*. 2001;58:302-307.
53. Zhao Q, Agger MP, Fitzpatrick M, et al. Cellular interactions with biomaterials: in vivo cracking of pre-stressed pellethane 2363-80A. *J Biomed Mater Res*. 1990;24:621-637.
54. Pinchuk L. Crack-resistant polycarbonate urethane polymer prostheses. Patent EP0461375B1, 1993.
55. Khan M, Yang J, Shi C, et al. Surface modification of polycarbonate urethane with Zwitterionic Polynorbornene via thiol-ene click-reaction to facilitate cell growth and proliferation. *Macromol Mater Eng*. 2015;300:802-809.
56. Geary C, Birkinshaw C, Jones E. Characterisation of Bionate polycarbonate polyurethanes for orthopaedic applications. *J Mater Sci Mater Med*. 2008;19:3355-3363.
57. Zare S, Kargari A. Membrane properties in membrane distillation. *Emerging Technologies for Sustainable Desalination Handbook*. 2018;1:107-156. Elsevier Inc.
58. Sophia Fox AJ, Bedi A, Rodeo SA. The basic science of articular cartilage: structure, composition, and function. *Sports Health*. 2009;1:461-468.
59. Park H, Park K, Shalaby WSW. Controlled release drug delivery systems. *Biodegradable Hydrogels for Drug Delivery*. 1993;1:1-6. Technomic Publishing Company.
60. Budianto E, Amalia A. Swelling behavior and mechanical properties of chitosan-poly(N-vinyl-pyrrolidone) hydrogels. *J Polym Eng*. 2020;40:551-560.
61. Bashir S, Teo YYIN, Ramesh S, Ramesh K, Rizwan M. Synthesis and characterization of pH-sensitive N-succinyl chitosan hydrogel and its properties for biomedical applications. *J Chil Chem Soc*. 2019;64:4571-4574.
62. Cornwell CF, Wille LT. Elastic properties of single-walled carbon nanotubes in compression. *Solid State Commun*. 1997;101:555-558.
63. Murakami T, Yarimitsu S, Nakashima K, et al. Superior lubricity in articular cartilage and artificial hydrogel cartilage. *Proc Inst Mech Eng Part J J Eng Tribol*. 2014;228:1099-1111.
64. Baker MI, Walsh SP, Schwartz Z, Boyan BD. A review of polyvinyl alcohol and its uses in cartilage and orthopedic applications. *J Biomed Mater Res - Part B Appl Biomater*. 2012;100 B:1451-1457.
65. Setton LA, Elliott DM, Mow VC. Altered mechanics of cartilage with osteoarthritis: human osteoarthritis and an experimental model of joint degeneration. *Osteoarthr Cartil*. 1999;7:2-14.
66. Little CJ, Bawolin NK, Chen X. Mechanical properties of natural cartilage and tissue-engineered constructs. *Tissue Eng - Part B Rev*. 2011;17:213-227.
67. Huang Y, Zheng Y, Song W, Ma Y, Wu J, Fan L. Poly(vinyl pyrrolidone) wrapped multi-walled carbon nanotube/poly(vinyl alcohol) composite hydrogels. *Compos Part A Appl Sci Manuf*. 2011;42:1398-1405.
68. Knapczyk-Korczak J, Zhu J, Ura DP, et al. Enhanced water harvesting system and mechanical performance from Janus fibers with polystyrene and cellulose acetate. *ACS Sustain Chem Eng*. 2021;9:180-188.
69. Kurokawa N, Hotta A. Regenerated cellulose nanofibers fabricated through electrospinning and saponification of cellulose acetate as reinforcement of polylactide composites. *Cellul*. 2019;26:7797-7808.
70. Lee DH, Jo MJ, Han SW, Yu S, Park H. Polyimide aerogel with controlled porosity: solvent-induced synergistic pore development during solvent exchange process. *Polymer*. 2020;205:122879.
71. Chen YS, Tsou PC, Lo JM, Tsai HC, Wang YZ, Hsiue GH. Poly(N-isopropylacrylamide) hydrogels with interpenetrating multiwalled carbon nanotubes for cell sheet engineering. *Biomaterials*. 2013;34:7328-7334.
72. Lan W, Zhang X, Xu M, et al. Carbon nanotube reinforced polyvinyl alcohol/biphasic calcium phosphate scaffold for bone tissue engineering. *RSC Adv Royal Soc Chemis*. 2019;9:38998-39010.
73. Ogawa T, Ding B, Sone Y, Shiratori S. Super-hydrophobic surfaces of layer-by-layer structured film-coated electrospun nanofibrous membranes. *Nanotechnology*. 2007;18:1-8.
74. Saifuddin N, Raziah AZ, Junizah AR. Carbon nanotubes: a review on structure and their interaction with proteins. *J Chem*. 2013;2013:1-18.
75. Wang B, Pang B. The influence of N,N-Dimethylformamide on dispersion of multi-walled carbon nanotubes. *Russ J Phys Chem A*. 2020;94:810-817.
76. Manorma FI, Alves P, Gil MH, Gando-Ferreira LM. Lignin separation from black liquor by mixed matrix polysulfone nanofiltration membrane filled with multiwalled carbon nanotubes. *Sep Purif Technol*. 2021;260:118231.
77. Yan Y, Xing J, Xu W, et al. Hydroxypropyl-β-cyclodextrin grafted polyethyleneimine used as transdermal penetration enhancer of diclofenac sodium. *Int J Pharm*. 2014;474:182-192.
78. Adepu S, Gaydhane MK, Kakunuri M, Sharma CS, Khandelwal M, Eichhorn SJ. Effect of micropatterning induced surface hydrophobicity on drug release from electrospun cellulose acetate nanofibers. *Appl Surf Sci*. 2017;426:755-762.
79. Ritger P, Peppas N. A simple equation for description of solute release I. Fickian and non-fickian release from non-swellable devices in the form of slabs, spheres, cylinders or discs. *J Control Release*. 1987;5:23-26.
80. Rezaei A, Nasirpour A. Evaluation of release kinetics and mechanisms of curcumin and curcumin-β-Cyclodextrin inclusion complex incorporated in electrospun almond gum/PVA nanofibers in simulated saliva and simulated gastrointestinal conditions. *Bionanoscience BioNanoScience*. 2019;9:438-445.
81. Şenel Ayaz HG, Perets A, Ayaz H, et al. Textile-templated electrospun anisotropic scaffolds for regenerative cardiac tissue engineering. *Biomaterials*. 2014;35:8540-8552.
82. Lukanina KI, Grigoriev TE, Krasheninnikov SV, Mamagulashvilli VG, Kamyshinsky RA, Chvalun SN. Multi-hierarchical tissue-engineering ECM-like scaffolds based on cellulose acetate with collagen and chitosan fillers. *Carbohydr Polym*. 2018;191:119-126.
83. Shrestha R, Palat A, Punnoose AM, Joshi S, Ponraju D, Paul SFD. Electrospun cellulose acetate phthalate nanofibrous scaffolds fabricated using novel solvent combinations biocompatible for primary chondrocytes and neurons. *Tissue Cell*. 2016;48:634-643.

SUPPORTING INFORMATION

Additional supporting information may be found in the online version of the article at the publisher's website.

How to cite this article: Oliveira AS, Ferreira I, Branco AC, et al. Development of polycarbonate urethane-based materials with controlled diclofenac release for cartilage replacement. *J Biomed Mater Res*. 2022;110(8):1839-1852. doi:10.1002/jbm.b.35042